Scientific Research Publishing

Atmospheric and Climate Sciences, 2026, 16(1), 190-209
https://www.scirp.org/journal/acs
ISSN Online: 2160-0422
ISSN Print: 2160-0414

Spatial Clustering Patterns of Thermal Extremes over Epochs in Douala, Littoral Region of Cameroon

Mbia Ekolok Awuh

Department of Geography and Planning, University of Bamenda (UBa), Bamenda, Cameroon
Email: awuhekolok@yahoo.co.uk

How to cite this paper: Awuh, M.E. (2026) Spatial Clustering Patterns of Thermal Extremes over Epochs in Douala, Littoral Region of Cameroon. *Atmospheric and Climate Sciences*, **16**, 190-209.
https://doi.org/10.4236/acs.2026.161012

Received: December 28, 2025
Accepted: January 19, 2026
Published: January 22, 2026

Abstract

This study analyzes the spatiotemporal evolution of thermal extremes in Douala, Cameroon, using Landsat-derived land surface temperature from 1994, 2004, 2014, and 2024. The author employed the Getis-Ord Gi* spatial statistic on 150 sampling points to identify statistically significant hot and cold spots. The findings reveal a transition from a compact heat island in 1994 (23 significant hotspots) to an extensive, polarized thermal landscape characterized by consolidated extreme heat in urbanized zones in 2024 (41 hot spots) and intensified cold spots in vegetated peripheries (17 in 1994 to 28 in 2024). The 99% confidence hot spots decreased from 14 (1994) to 10 (2024), indicating consolidation of extreme heat (32.3˚C - 34.3˚C). The extreme thermal polarization suggests Douala needs targeted policies to balance urban development with thermal comfort, to reduce health disparities, and improve the environmental quality in Douala. To mitigate the extreme polarization in Douala, this study recommends that urban planners should prioritize green spaces in hotspots, preserve peripheral vegetation, and encourage sustainable urban designs.

Keywords

Thermal Extremes, Hot Spot, Cold Spot, Analysis, LST Spatial Cluster, Land Cover

1. Introduction

Most urban areas have been dramatically extended during the past decades due to urbanization [1]. This urban growth dynamic is not uniform, and urban expansion patterns differ significantly globally [2]. According to [3], the number of people living in urban areas will increase by 2.5 billion by 2050, with nearly 90% of

this growth happening in Asia and Africa. At the same time, thermal extremes show significant spatial clustering patterns, forming localized "hot spots" and "cold spots" driven primarily by land use, urban morphology, geographic location, and climate change. The UHI effect has become one of the clearest examples of how urbanization affects the local and regional climate [4]. Urban areas change the albedo and nocturnal radiation [5] [6], while urban transportation contributes to greenhouse gas emissions that are likely to increase the local temperature [7]. Emerging cities will be hotspots of heat-related risks from climate change, as modification and changes in land use and land cover (LULC) intensify the urban heat island (UHI) effect, and subsequently, exacerbate current and projected heat stress [8]-[11].

There are various parameters describing the dynamics of the urban thermal environment. Surface temperature is the temperature at a surface, which is often used to examine heat exposure in multi-city studies and for informing urban heat mitigation efforts due to the scarcity of urban air temperature measurements [12]. LST is the temperature at the land surface; due to limitations in observation and modeling, LST is often used to measure the urban heat island effects [13] [14]. Surface and Air urban heat intensity have been observed in different ways; air UHI is based on the air temperature, based on site monitoring, and the SUHI is based on the surface temperature data collected by remote sensing images [15]. LST is the temperature at the land surface; due to limitations in observation and modeling, LST is often used as a proxy for urban heat stress [13]. The growth of cities has been predicted to continue, and successfully managing city growth will be critical to economic development and social stability [16]. This study aims to investigate the patterns of thermal characteristics over Douala.

2. Materials and Methods

2.1. Study Area

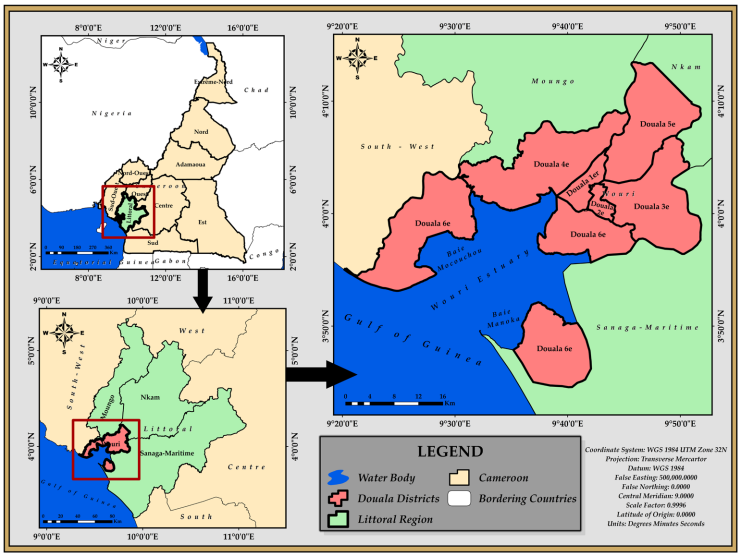

Figure 1. Location of Douala.

Douala is the economic capital and largest city in Cameroon. The city is located on the Atlantic Ocean coast, between 4˚03' North latitude and 9˚42' East longitude, with an area of about 210 km^2 (**Figure 1**). The city has an equatorial climate with temperatures ranging from 18˚C to 34˚C and high humidity (80% - 99%) evenly distributed throughout the year.

2.2. Land Surface Temperature Retrieval

Land surface temperature (LST) was retrieved from Landsat thermal infrared data using the single-channel algorithm, which converts at-sensor brightness temperature to land surface temperature through atmospheric correction and emissivity adjustment. For Landsat 5 TM, 7 ETM+ (1994, 2004) and Landsat 8 OLI/TIRS (2014, 2024), the thermal band digital numbers were first converted to at-sensor spectral radiance using radiometric calibration coefficients from the metadata files, then transformed to at-sensor brightness temperature using the inverse Planck function with band-specific calibration constants. Land surface emissivity (ε) was estimated using the Normalized Difference Vegetation Index (NDVI) threshold method, and mixed categories with emissivity calculated through linear interpolation based on NDVI values and proportional vegetation cover. Atmospheric transmittance, upwelling radiance, and downwelling radiance parameters required for atmospheric correction were obtained from the NASA Atmospheric Correction Parameter Calculator using time-specific and location-specific atmospheric profiles, which were then integrated into the single-channel algorithm to derive final land surface temperature values in degrees Celsius. The single-channel method was selected over split-window algorithms because Landsat 5 TM has only one functional thermal band, and to maintain methodological consistency across all observation years, despite Landsat 7 ETM+ and 8 TIRS having two thermal bands.

2.3. Hot Spot Detection

The Getis-Ord Gi* spatial statistic was applied to identify statistically significant thermal hot spots and cold spots in the land surface temperature distribution across Douala for each observation year (1994, 2004, 2014, and 2024). The Getis-Ord Gi* statistic provides a robust spatial statistical method for detecting significant hot spots and cold spots, distinguishing clustered thermal extremes from randomly distributed temperature variations [17]. This approach has been widely applied in urban heat island research to identify neighborhoods requiring priority intervention and evaluate the spatial extent of thermal stress zones [18]-[20]. This methodology allowed for the identification of thermal clustering patterns that distinguish genuine spatial autocorrelation from random temperature variations, providing robust evidence of urban heat island structure and evolution across the thirty-year study period.

A total of 150 sampling points were generated across the study area using the

Create Fishnet tool to establish an evenly distributed grid pattern. Land surface temperature values were extracted at each sampling point location from the LST maps derived from Landsat thermal infrared data, creating a point dataset of temperature observations that served as input for the spatial statistical analysis. LST values for each observation year were extracted to these point locations using the Extract Multi Values to Points tool, creating point feature classes containing temperature attributes for each observation year. The selection of 150 evenly distributed sampling points for the Getis-Ord Gi* hotspot analysis represents a balance between computational efficiency, statistical robustness, and the metropolitan-scale analytical objectives of the research, while acknowledging certain limitations in capturing fine-scale microclimatic variations. The spatial resolution of approximately one sampling point per 6.3 km^2 (based on the study area extent of ~950 km^2) is appropriate for identifying regional-scale thermal clustering patterns and urban heat island structure at the metropolitan level, which is a primary focus of this research, and is likely consistent with similar hotspot analyses in urban climate studies examining city-wide thermal patterns rather than neighborhood-scale variations. The 150-point density ensures adequate spatial coverage across all land cover types, geographical divisions, and thermal zones while maintaining sufficient point distribution to satisfy the spatial statistical requirements of the Getis-Ord Gi* statistic, which requires each point to have neighboring observations within the specified search radius for calculating local spatial autocorrelation.

The Getis-Ord Gi* statistic was calculated for each sampling point to determine whether the temperature at that location, along with temperatures at neighboring points within a defined search radius, exhibited statistically significant spatial clustering of high values (hot spots) or low values (cold spots) compared to the random distribution expected under the null hypothesis of spatial independence. The analysis produced z-scores and p-values for each point, with statistically significant hot spots identified at three confidence levels: 90% confidence (z-score > 1.65), 95% confidence (z-score > 1.96), and 99% confidence (z-score > 2.58), while cold spots were identified at corresponding negative z-score thresholds: 90% confidence (z-score < −1.65), 95% confidence (z-score < −1.96), and 99% confidence (z-score < −2.58). Points with z-scores falling between −1.65 and +1.65 were classified as "not significant," indicating that temperatures at those locations did not exhibit statistically significant spatial clustering.

3. Spatial and Temporal Patterns of Temperature Distribution

The land surface temperature trend analysis of Douala from 1994 to 2024 (**Figure 2**) reveals a consistent and substantial warming pattern across all temperature metrics, providing quantitative evidence of the thermal impacts associated with urbanization and vegetation loss (**Figure 3**).

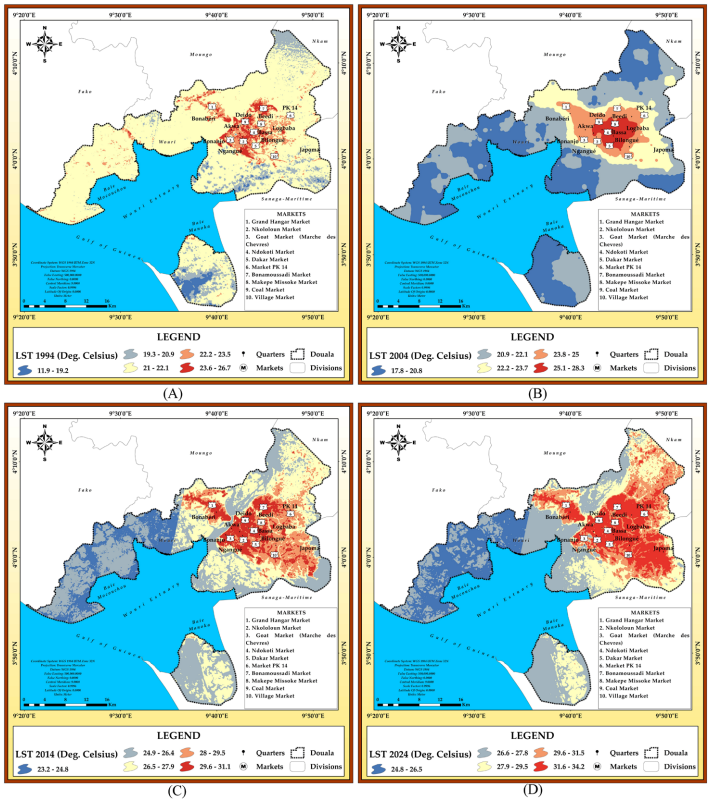

Figure 2. Spatial and temporal patterns of temperature distribution in Douala.

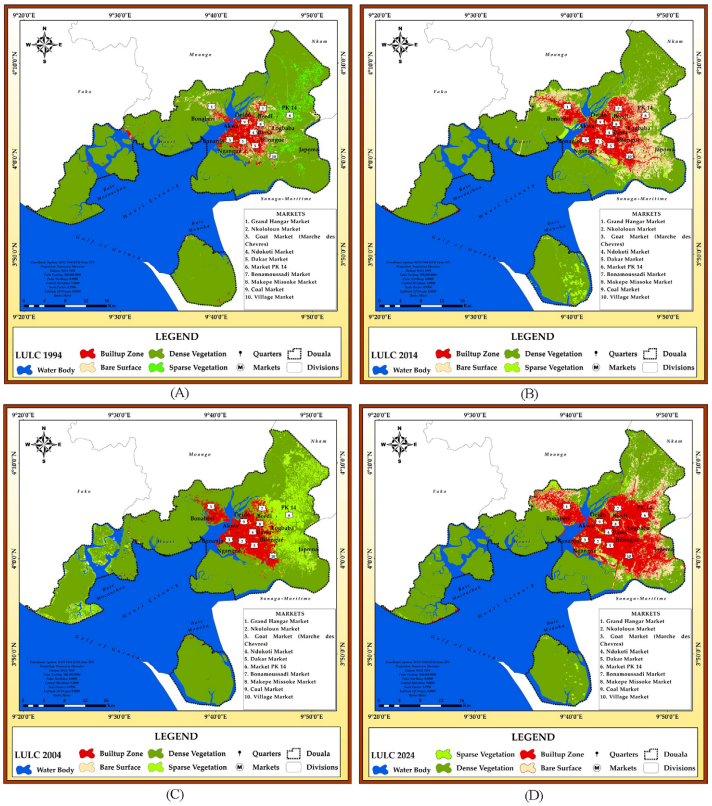

Figure 3. LULC dynamics in Douala.

3.1. Hot Spot Analysis for 1994

The hotspot analysis for the 1994 land surface temperature (Figure 4 and Figure 5) reveals a thermal landscape characterized by minimal statistically significant clustering, with the vast majority of the study area (110 locations or 73% of 150 sampling points) classified as "not significant".

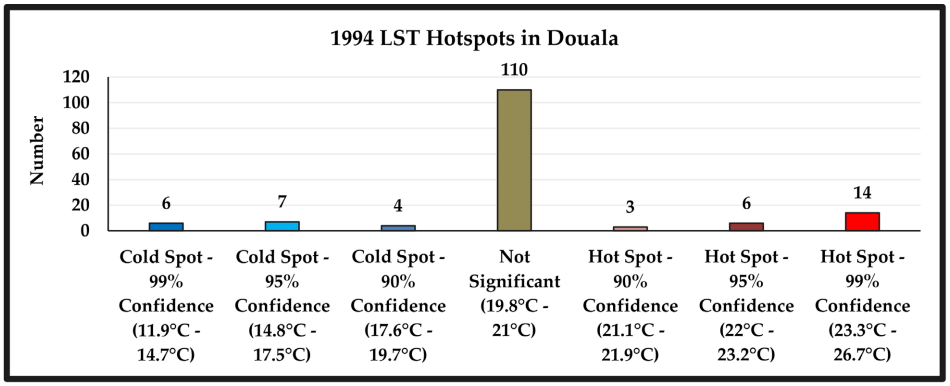

Figure 4. Distribution of 1994 LST hotspots in Douala.

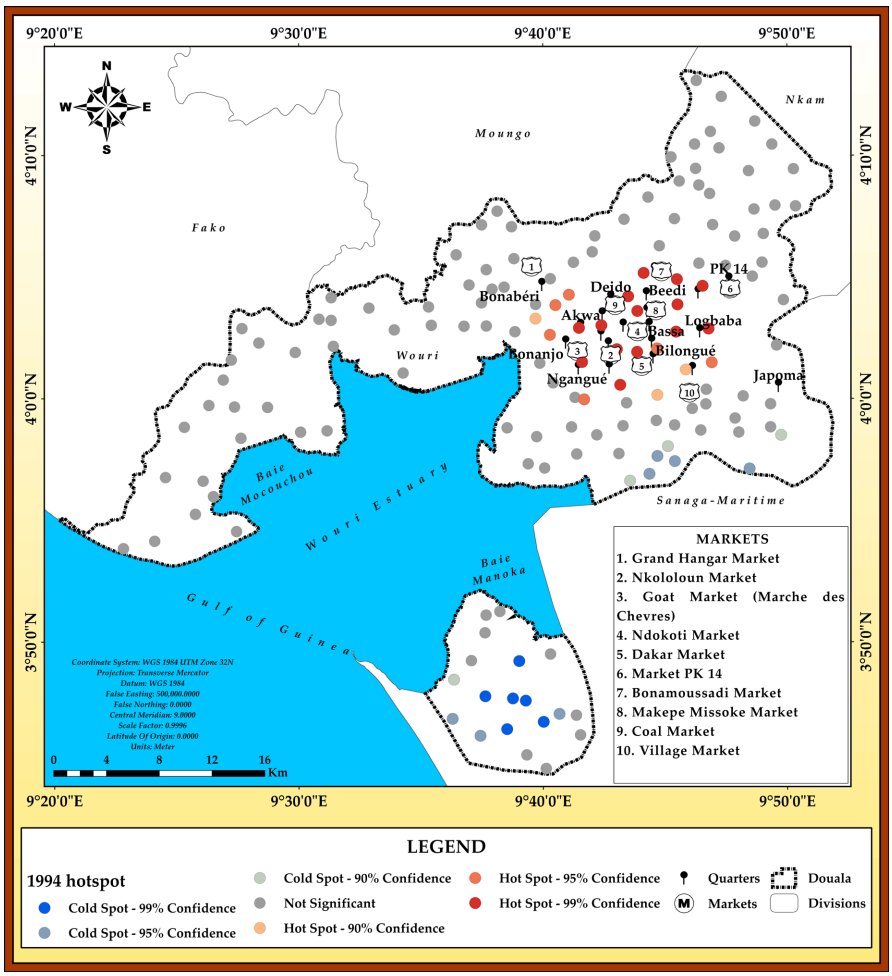

Figure 5. Spatial distribution of 1994 LST hotspots in Douala.

The thermal characteristics, as depicted in Figure 4 and Figure 5, indicate relatively homogeneous thermal conditions across Douala during the baseline 1994 period when vegetation dominated 80% of the landscape. The analysis identified only 14 statistically significant hot spots at 99% confidence (23.3˚C - 26.7˚C), representing locations with relatively high temperatures that were surrounded by similarly warm areas, thus forming clustered thermal hotspots primarily associated with the compact urban core. An additional 6 hot spots were detected at 95% confidence (22˚C - 23.2˚C) and 3 at 90% confidence (21.1˚C - 21.9˚C), representing moderate thermal clustering in transitional peri-urban zones. On the cooling end of the spectrum, the analysis detected minimal cold spot clustering with only 4 locations at 90% confidence (17.6˚C - 19.7˚C), 7 at 95% confidence (14.8˚C - 17.5˚C), and 6 at 99% confidence (11.9˚C - 14.7˚C), totaling just 17 statistically significant cold spots compared to 23 hot spots, suggesting that while cool temperatures were widespread throughout the vegetated periphery, intense cold spot clustering was limited to specific locations, likely water bodies and particularly dense vegetation stands. The dominance of non-significant locations (110 out of 150 sampling points) indicates that in 1994, the thermal environment of Douala was characterized by moderate, relatively uniform temperatures across most of the metropolitan area. The limited spatial clustering of extreme heat or cold reflects the extensive vegetation cover that provided widespread cooling and the small, compact urban core (54.2 km^2 as shown in Figure 1) that generated localized but not extensive thermal hotspots.

The spatial distribution of statistically significant LST hotspots in 1994 (Figure 4) reveals a compact, well-defined urban heat island concentrated exclusively in the central business district, with hot spots forming a distinct cluster in the traditional urban core, while cold spots appeared scattered throughout the peripheral vegetated areas and southern water body regions. The 99% confidence hot spots were tightly concentrated in the Akwa-Bonanjo-Deido axis, forming the thermal nucleus of the metropolitan area and corresponding precisely with the built-up zone documented in the 1994 LULC map (Figure 1), with additional hot spots appearing in New Bell, Bali, and portions of Bonaberi where the most intensive urban development and market activities occurred, including areas around Grand Hangar Market, Nkolotoun Market, and central commercial districts. The 95% and 90% confidence hot spots formed a transitional thermal buffer surrounding the core, appearing in periurban neighborhoods such as Bessengue, Bonapriso, and areas approaching Logbaba and Ndogpassi, representing locations where mixed urban-vegetation land covers produced moderate thermal clustering. The 99% confidence cold spots (dark blue circles) appeared predominantly in the southern division toward Sanaga-Maritime and in association with water bodies, including portions of Baie Manoka, where the cooling influence of the ocean, estuarine waters, and intact coastal vegetation created statistically significant cool zones surrounded by similarly cool areas. The 95% and 90% confidence cold spots were distributed throughout the eastern, western, and northern peripheral divisions to-

ward Moungo and Nkam, appearing in areas of dense vegetation cover that provided localized cooling effects. The spatial pattern reveals clear thermal zoning with a compact hot spot cluster occupying less than 10% of the study area in the urban core, surrounded by extensive non-significant zones, which represent the moderate temperatures that characterized most of the vegetated landscape. Alongside the scattered cold spots in peripheral areas, these establish a baseline thermal geography characterized by a small, isolated urban heat island surrounded by a vast, relatively cool vegetated periphery.

3.2. Hot Spot Analysis for 2004

An additional 7 hot spots were detected at 95% confidence (24.3˚C - 25.3˚C) and 2 at 90% confidence (23.5˚C - 24.2˚C), totaling 28 statistically significant hot spots in 2004 compared to 23 in 1994 (Figure 6 and Figure 7), confirming the spatial expansion of thermal clustering associated with urban growth. Furthermore, the analysis revealed a notable increase in cold spot clustering with 13 locations at 90% confidence (21.5˚C - 22.3˚C), representing over a threefold increase from the 4 cold spots detected at this confidence level in 1994, and 6 locations at 95% confidence (20.3˚C - 21.4˚C).

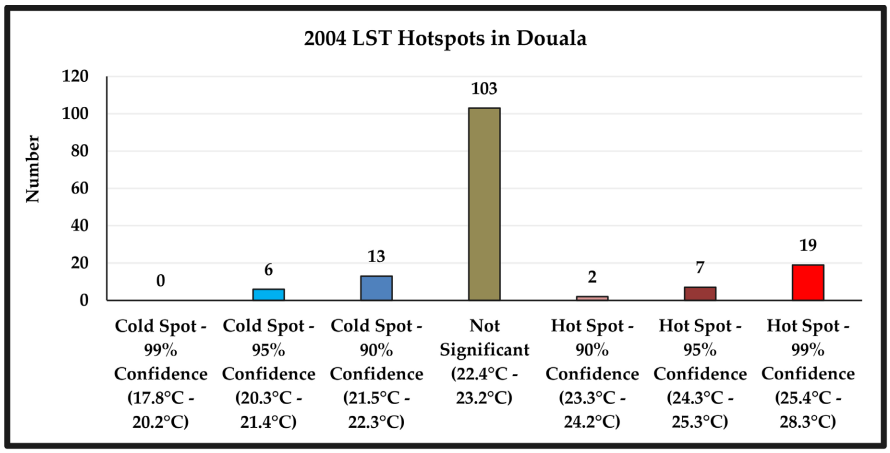

Figure 6. Distribution of 2004 LST hotspots in Douala.

The cold spot pattern changed dramatically from 1994, with 90% and 95% confidence cold spots now distributed more extensively throughout the northern divisions toward Nkam, western areas toward Moungo, and southern regions approaching Sanaga-Maritime, mostly appearing in both vegetated peripheries and water body locations. No cold spots were detected at 99% confidence (17.8˚C - 20.2˚C), suggesting that the most intense cold spot clustering observed in 1994 had diminished or fragmented by 2004, possibly due to vegetation loss, edge effects from encroaching urbanization, or warming of previously cool areas. The total of 19 cold spots in 2004 compared to 17 in 1994 represents a modest increase, but the shift in confidence levels with more cold spots at lower confidence thresholds and none at the highest confidence suggests that cold spot clustering became

less intense and more spatially diffused as vegetation cover declined from 80% to 66% of the study area (Figure 2(A) and Figure 2(B)). The slight decrease in non-significant locations from 110 to 103, combined with increases in both hot and cold spot counts, indicates emerging thermal polarization where the landscape exhibited greater spatial clustering of both extreme heat and relative coolness, further reflecting the documented expansion of both built-up areas (to 87.3 km^2) and sparse vegetation (to 143.0 km^2) documented in Figure 2(B).

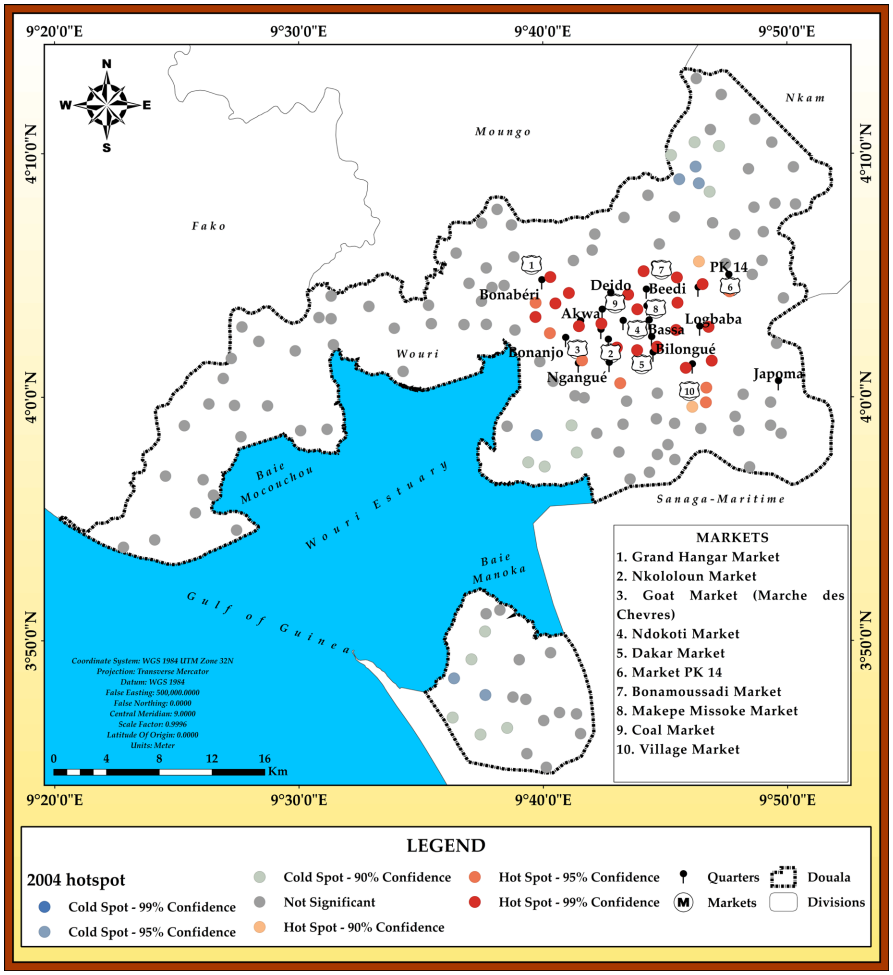

Figure 7. Spatial distribution of 2004 LST hotspots in Douala.

The spatial distribution of statistically significant LST hotspots in 2004 (Figure 7) reveals an expanded urban heat island with hot spots spreading outward from the 1994 core into newly urbanized neighborhoods, while cold spots exhibited increased but distributed clustering in peripheral vegetated areas, reflecting a decade of urban expansion and landscape transformation. The 99% confidence hot spots expanded beyond the compact 1994 core, now forming a larger clustered zone that encompasses New Bell, Bali, Bessengue, portions of Logbaba, areas around Ndokoti Market and Dakar Market, and extending into Bonaberi, Bonapriso, and neighborhoods approaching Ndogpassi. This corresponds with the built-up ex-

pansion documented in the 2004 LULC map (Figure 2(B)), where urban development extended along major transportation corridors radiating from the central business district. The 95% and 90% confidence hot spots appeared in the expanding periurban fringe, including areas around Bonamoussadi, portions of PK 14, and transitional zones in the northeastern expansion corridor, representing newly urbanizing areas that had not yet achieved the thermal intensity of the urban core but exhibited statistically significant warming compared to surrounding areas.

The cold spot pattern changed dramatically from 1994, with 90% and 95% confidence cold spots now distributed more extensively throughout the northern divisions toward Nkam, western areas toward Moungo, and southern regions approaching Sanaga-Maritime, mostly appearing in both vegetated peripheries and water body locations. No 99% confidence cold spots were detected anywhere in the study area, confirming the quantitative finding in Figure 4 that intense cold spot clustering had disappeared by 2004, likely due to regional warming, vegetation fragmentation, or reduced cooling capacity of remaining natural areas affected by edge effects from surrounding development.

The spatial pattern reveals an expanding hot spot cluster that now occupied approximately 15% - 20% of the study area compared to less than 10% in 1994, with hot spots spreading in multiple directions from the core, particularly eastward and northeastward along the main urban expansion vectors, while cold spots became more numerous but less intensely clustered, distributed throughout peripheral areas but lacking the strong cooling signatures observed in 1994.

3.3. Hot Spot Analysis for 2014

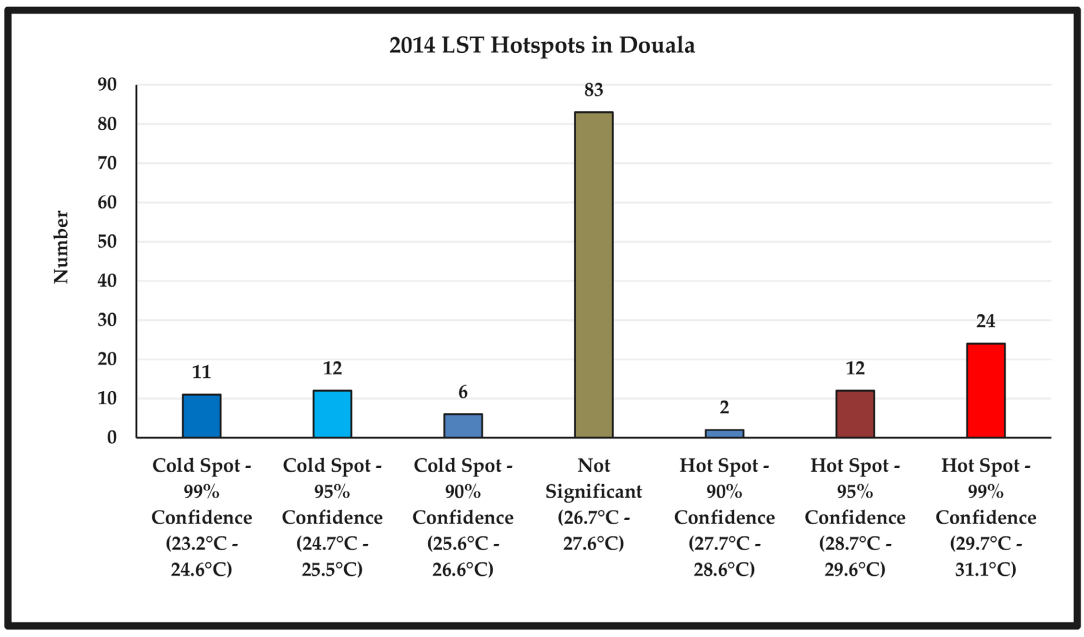

Figure 8. Distribution of 2014 LST hotspots in Douala.

Furthermore, the hotspot analysis for 2014 land surface temperature (Figure 8

and Figure 9) reveals dramatic thermal polarization with substantial increases in both hot and cold spot clustering, indicating that the metropolitan thermal environment had become increasingly heterogeneous and characterized by extreme spatial contrasts between intensely hot urban zones and relatively cool peripheral areas.

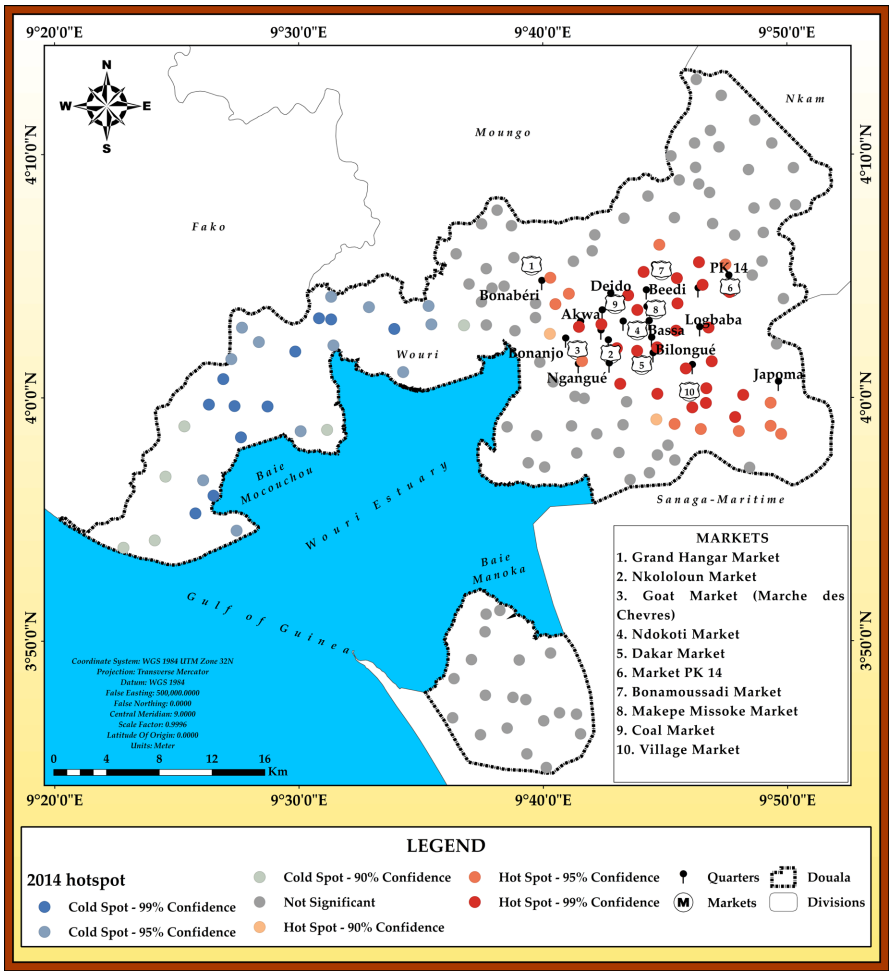

Figure 9. Spatial distribution of 2014 LST hotspots in Douala.

The analysis (Figure 8 and Figure 9) identified 24 statistically significant hot spots at 99% confidence (29.7˚C - 31.1˚C), representing a 26% increase from 2004 and a 71% increase from 1994. This demonstrates progressive expansion and intensification of extreme heat clustering corresponding with urban expansion to 111.5 km^2 (Figure 2(C)). Additionally, 12 hot spots were detected at 95% confidence (28.7˚C - 29.6˚C) and 2 at 90% confidence (27.7˚C - 28.6˚C), totaling 38 statistically significant hot spots. In contrast, cold spot clustering increased more dramatically, with 11 locations at 99% confidence (23.2˚C - 24.6˚C), 12 at 95% confidence (24.7˚C - 25.5˚C), and 6 at 90% confidence (25.6˚C - 26.6˚C).

Meanwhile, the non-significant category declined to 83 locations (55% of sam-

pling points), indicating moderate temperatures now characterize only about half the study area. Consequently, the combined total of 67 statistically significant hot and cold spots in 2014 demonstrates increasing thermal polarization and spatial structure. The spatial distribution of LST hotspots in 2014 (Figure 8) revealed a dramatically expanded urban heat island with hot spots forming a massive cluster across the eastern half of the metropolitan area. Cold spots exhibited strong clustering throughout western and southern peripheral areas, establishing a clear east-west thermal gradient.

The 99% confidence hot spots formed a nearly continuous cluster encompassing the central and eastern urbanized area (Akwa, Bonanjo, Deido, New Bell, Bali, Bessengue, Bassa, Logbaba, Bilongue, Ndogpassi) and extending far into the eastern expansion corridor toward Japoma and well beyond PK 14 corresponding with the built-up concentration documented in the 2014 LULC map (Figure 3(C)) and represents a hot spot zone that now occupied approximately 30% - 40% of the study area compared to 15% - 20% in 2004 and less than 10% in 1994. The 95% and 90% confidence hot spots appeared at the periphery of this massive hot cluster and formed a transitional thermal fringe in areas such as Bonamoussadi, with scattered locations in the eastern periphery where urbanization was actively progressing, thus representing locations that were warming but had not yet achieved the extreme clustering intensity of the urban core.

The cold spot pattern showed dramatic transformation, with 99% confidence cold spots forming strong clusters throughout western divisions and in the southern division approaching Sanaga-Maritime. As a result, the spatial pattern establishes a polarized thermal geography with an enormous hot spot cluster dominating the urbanized central-eastern half of Douala and substantial cold spot clusters throughout the vegetated western periphery.

3.4. Hot Spot Analysis for 2024

By 2024, the hotspot analysis for LST in Douala (Figure 10 and Figure 11) revealed continued but slightly moderated thermal clustering compared to 2014, with cold spots showing dramatic intensification while hot spots remained extensive, further establishing a thermal landscape characterized by extreme spatial polarization.

The analysis (Figure 10) identified 10 statistically significant hot spots at 99% confidence (32.4˚C - 34.2˚C), representing a 58% decrease from the 24 hot spots detected in 2014, though these remaining hot spots exhibited even higher absolute temperatures (32.4˚C - 34.3˚C compared to 29.7˚C - 31.1˚C in 2014), suggesting spatial consolidation of extreme heat into fewer but more intensely hot clustered zones (Figure 10). An additional 21 hot spots were detected at 95% confidence (30.8˚C - 32.3˚C) and 10 at 90% confidence (29.5˚C - 30.7˚C), totaling 41 statistically significant hot spots in 2024 compared to 38 in 2014. This indicates that overall hot spot extent remained extensive, though the spatial configuration shifted, with fewer extreme clusters at the highest confidence level

but more moderate clustering at lower thresholds, possibly reflecting the conversion of bare surface to built-up area between 2014 and 2024, which reduced thermal heterogeneity within urbanized zones while maintaining extensive elevated temperatures. Cold spot clustering intensified dramatically, with 26 locations at 99% confidence (24.8˚C - 26.1˚C), more than doubling from the 11 detected in 2014 and representing the strongest cold spot clustering observed across the entire study period, This finding is suggesting that peripheral vegetated areas and water bodies, now increasingly isolated and distant from the expanding urban core, functioned as powerful cooling refuges providing statistically significant temperature moderation.

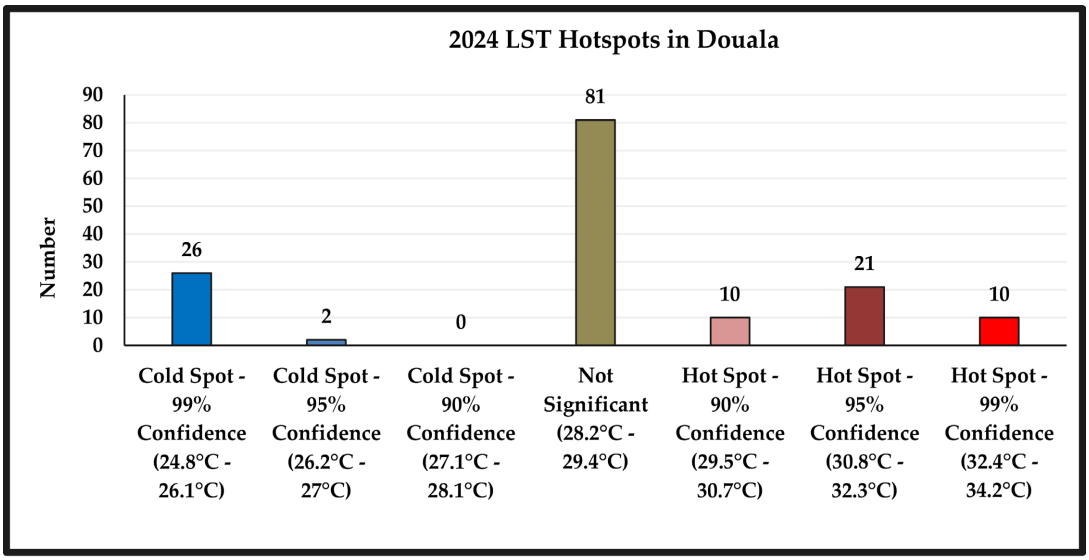

Figure 10. Distribution of 2024 LST hotspots in Douala.

Additionally, 2 cold spots (Figure 10) were detected at 95% confidence (26.2˚C - 27.0˚C), but remarkably, no cold spots were detected at 90% confidence (27.1˚C - 28.1˚C), indicating a highly concentrated cold spot pattern with strong clustering at the highest confidence level but minimal transitional cooling zones. The non-significant category declined further to 81 locations (54% of sampling points), essentially unchanged from the 83 (55%) observed in 2014, confirming that thermal polarization and spatial clustering remained the dominant characteristic of Douala's thermal landscape. The combined total of 69 statistically significant hot and cold spots compared to 67 in 2014 indicates that overall thermal clustering remained extensive. However, the distribution shifted dramatically with cold spots dominating (28 total compared to 29 in 2014) while hot spots remained substantial (41 compared to 38 in 2014), thus establishing a thermal landscape characterized by extreme spatial differentiation between heat-generating urban zones and cooling natural areas. Subsequently, the spatial distribution of statistically significant LST hotspots in 2024 (Figure 11) reveals a consolidated but extremely intense urban heat island.

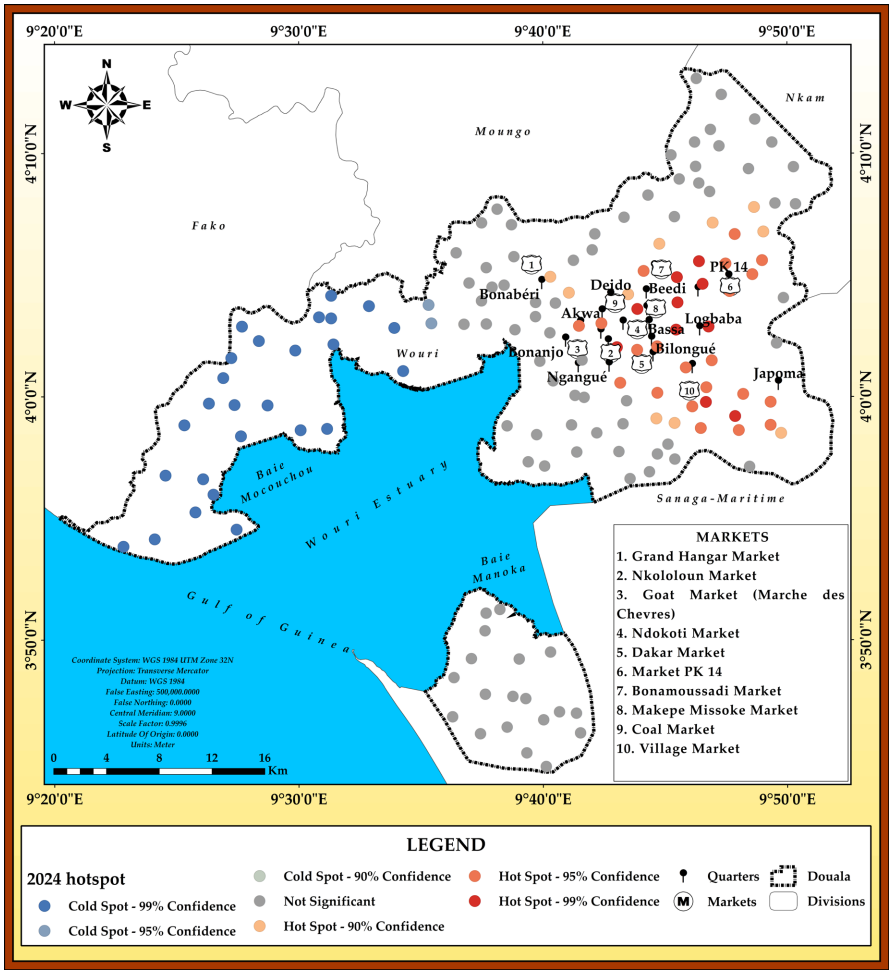

Figure 11. Spatial distribution of 2024 LST hotspots in Douala.

The most extreme hot spots are concentrated in the central and eastern urban core, while cold spots formed an extensive, intensely clustered cooling zone throughout the western peripheral divisions, establishing the most spatially polarized thermal geography observed across the entire study period. The 99% confidence hot spots, though reduced in number compared to 2014, formed a concentrated cluster in the densest portions of the urbanized area, including central Akwa, Bonanjo, Deido, New Bell, Bessengue, Bassa, Logbaba, and major market centers. These locations where extremely high temperatures were surrounded by similarly extreme heat, creating a thermal core of exceptional intensity. The 95% and 90% confidence hot spots expanded this thermal zone extensively throughout the eastern urbanized region, encompassing Bilongue, Ndogpassi, extensive areas around and beyond PK 14, portions of Japoma, and the northeastern expansion corridor toward Bonamoussadi. This formed a massive hot spot region that occupied much of the eastern half of the study area and corresponded precisely with the extensive built-up zone (194.6 km^2) documented in the 2024 LULC map (**Figure 3(D)**). The cold spot pattern showed remarkable intensification, with 99% confidence cold spots forming an extensive, nearly continuous cluster throughout the western di-

visions toward Moungo, appearing in virtually all areas retaining dense vegetation and representing the strongest cold spot clustering observed across all observation periods. This suggests that these peripheral vegetated areas functioned as highly effective cooling zones providing statistically significant temperature moderation in stark contrast to the surrounding thermal environment. The 95% confidence cold spots extended this cooling region into additional western peripheral areas, while cold spots also appeared in association with water bodies in the southern division and portions of the northern periphery where vegetation persisted. The spatial pattern establishes extreme thermal polarization with a massive hot spot zone further dominating the urbanized central-eastern portion of the study area, an equally extensive cold spot zone throughout the vegetated western periphery, and minimal overlap or transitional zones between these thermal extremes. This has created a metropolitan landscape characterized by sharp thermal boundaries and extreme spatial differentiation with profound implications for thermal comfort, health equity, and quality of life. Figure 12 shows the distribution of hotspots in Douala from 1994 to 2024.

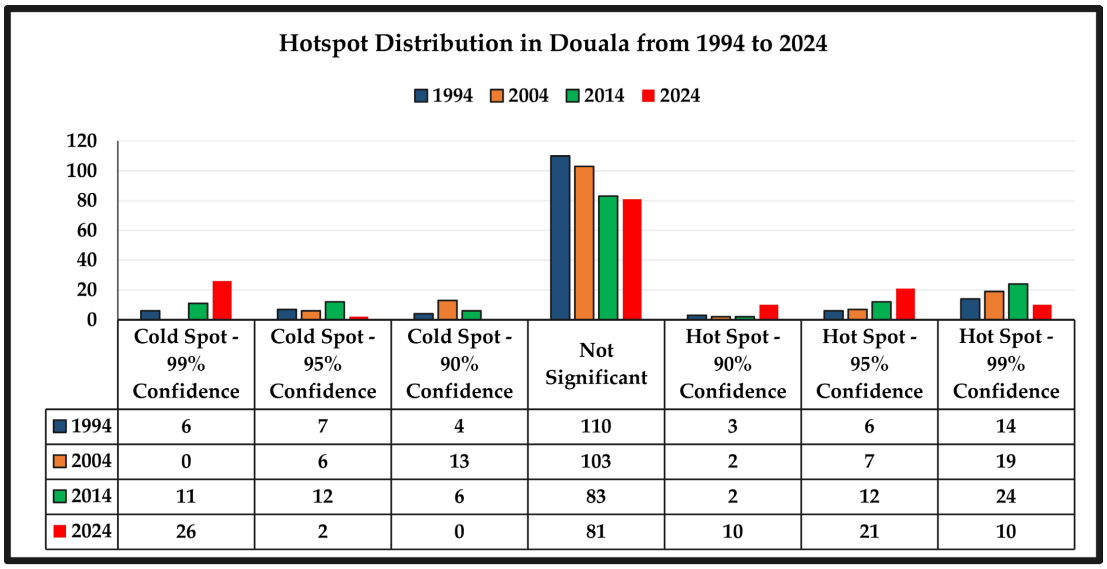

	Cold Spot - 99% Confidence	Cold Spot - 95% Confidence	Cold Spot - 90% Confidence	Not Significant	Hot Spot - 90% Confidence	Hot Spot - 95% Confidence	Hot Spot - 99% Confidence
1994	6	7	4	110	3	6	14
2004	0	6	13	103	2	7	19
2014	11	12	6	83	2	12	24
2024	26	2	0	81	10	21	10

Figure 12. Hotspot distribution in Douala from 1994 to 2024.

4. Discussion

The hotspot analysis reveals a dramatic shift in Douala's thermal environment. Hot spots tend to increase through time (from 23 hot spots in 1994 to 41 in 2024) and strongly correlate with urban expansion. Similar findings have been reported by [21]-[27]. The UHI effect is also strongly affected by the type of urban development. For instance, several authors have shown that not only the presence but also the spatial arrangement of vegetation has an impact on the cooling effect of vegetation land cover on the urban climate [28]. As urbanization increases, vegetation's spatial configuration will change, potentially impacting LST [29].

City size has been linked to the degree of UHI [30] [31]. Local climatic factors

like insolation, wind patterns, and time of day also contribute to changes in LST. Higher air temperatures contribute to increasing LST, leading to urban heat islands and adverse effects on human health and energy consumption. The reduction in 99% confidence hot spots from 14 in 2014 to 10 in 2024 suggests spatial consolidation of extreme heat into fewer but more intense zones, with temperatures reaching 32.4˚C - 34.3˚C (vs 29.7˚C - 31.1˚C in 2014). This indicates increasing thermal polarization. Similar findings have been reported by [23] [24] [32]-[36]. Simultaneously, cold spots intensified in peripheral vegetated areas, increasing from 17 in 1994 to 28 in 2024, establishing extreme thermal polarization. The decline in thermally non-significant areas from 73% (110 locations) in 1994 to 54% (81 locations) in 2024 confirms increasing thermal heterogeneity and the emergence of distinct, spatially clustered zones of extreme heat and relative coolness, replacing the previously moderate, homogeneous thermal landscape that characterized the vegetation-dominated 1994 baseline. Similar patterns have been seen in [37]-[40] where urban growth drives thermal heterogeneity.

Several studies have shown that increased thermal polarization increases the risk of heat-related diseases and mortality [41]-[44]. The vulnerability to heat in most urban centers has increased due to urbanization. For instance, [45] identified outdoor thermal discomfort in densely built-up areas, while [46] and [34] found heat stress and thermal discomfort to be the major health issues during the dry season. [34] reported that increasing temperatures have exacerbated heatstroke, heat stress, heat cramps, and dehydration.

5. Conclusion

This study analyzes the spatiotemporal evolution of thermal extremes in Douala. The thermal landscape of Douala shows a profound transformation from 1994 to 2024, with far-reaching implications. Hot spots have increased, correlating strongly with urban expansion and highlighting the growing intensity of the urban heat island effect. Cold spots have intensified in peripheral vegetation areas, establishing a stark contrast between urban and natural environments. Extreme thermal polarization has emerged, with hot zones dominating the central-eastern areas and cool zones prevailing in the western peripheries, creating a mosaic of thermal experiences across the city. Thermally non-significant areas have declined, indicating increasing thermal heterogeneity and a more complex urban thermal environment. To mitigate the extreme polarization in Douala, urban planners should prioritize green spaces in hotspots by increasing vegetation cover in the central-eastern areas to mitigate extreme heat (32.4˚C - 34.3˚C zones), protect and expand green belts around the city to maintain cool zones. Cooler areas with vegetation can promote better air quality and mental well-being. Also, urban planners should encourage sustainable urban designs.

Conflicts of Interest

The author declares no conflicts of interest regarding the publication of this paper.

References

[1] Mohan, R. and Dasgupta, S. (2004) Urban Development in India in the Twenty First Century: Policies for Accelerating Urban Growth. Working Paper No. 231. https://kingcenter.stanford.edu/sites/g/files/sbiybj16611/files/media/file/231wp_0.pdf

[2] Gollin, D., Jedwab, R. and Vollrath, D. (2016) Urbanization with and without Industrialization. *Journal of Economic Growth*, **21**, 35-70. https://doi.org/10.1007/s10887-015-9121-4

[3] DESA (2018) 2018 Revision of World Urbanization Prospects. https://www.un.org/en/desa/2018-revision-world-urbanization-prospects

[4] Chapman, S., Watson, J.E.M., Salazar, A., Thatcher, M. and McAlpine, C.A. (2017) The Impact of Urbanization and Climate Change on Urban Temperatures: A Systematic Review. *Landscape Ecology*, **32**, 1921-1935. https://doi.org/10.1007/s10980-017-0561-4

[5] Offerle, B., Jonsson, P., Eliasson, I. and Grimmond, C.S.B. (2005) Urban Modification of the Surface Energy Balance in the West African Sahel: Ouagadougou, Burkina Faso. *Journal of Climate*, **18**, 3983-3995. https://doi.org/10.1175/jcli3520.1

[6] Luo, M. and Lau, N. (2018) Increasing Heat Stress in Urban Areas of Eastern China: Acceleration by Urbanization. *Geophysical Research Letters*, **45**, 13060-13069. https://doi.org/10.1029/2018gl080306

[7] Grimmond, S. (2007) Urbanization and Global Environmental Change: Local Effects of Urban Warming. *The Geographical Journal*, **173**, 83-88. https://doi.org/10.1111/j.1475-4959.2007.232_3.x

[8] Oke, T.R. (1973) City Size and the Urban Heat Island. *Atmospheric Environment* (1967), **7**, 769-779. https://doi.org/10.1016/0004-6981(73)90140-6

[9] Awuh, M.E. (2021) Monitoring Day and Night-Time Situation of Urban Heat Island and Possible Adaptation Measures in Douala, Cameroon. *Journal of Geoscience and Environment Protection*, **9**, 163-176. https://doi.org/10.4236/gep.2021.98011

[10] Georgescu, M., Moustaoui, M., Mahalov, A. and Dudhia, J. (2013) Summer-Time Climate Impacts of Projected Megapolitan Expansion in Arizona. *Nature Climate Change*, **3**, 37-41. https://doi.org/10.1038/nclimate1656

[11] Li, Y., Schubert, S., Kropp, J.P. and Rybski, D. (2020) On the Influence of Density and Morphology on the Urban Heat Island Intensity. *Nature Communications*, **11**, 2647-2647. https://doi.org/10.1038/s41467-020-16461-9

[12] Mushore, T.D., Mutanga, O., Odindi, J. and Dube, T. (2017) Linking Major Shifts in Land Surface Temperatures to Long Term Land Use and Land Cover Changes: A Case of Harare, Zimbabwe. *Urban Climate*, **20**, 120-134. https://doi.org/10.1016/j.uclim.2017.04.005

[13] Orimoloye, I.R., Mazinyo, S.P., Nel, W. and Kalumba, A.M. (2018) Spatiotemporal Monitoring of Land Surface Temperature and Estimated Radiation Using Remote Sensing: Human Health Implications for East London, South Africa. *Environmental Earth Sciences*, **77**, Article No. 77. https://doi.org/10.1007/s12665-018-7252-6

[14] Awuh, M.E., Officha, M.C., Okolie A.O. and Enete, I.C. (2018) A Remote Sensing Analysis of the Temporal and Spatial Changes of Land Surface Temperature in Calabar Metropolis, Nigeria. *Journal of Geographic Information System*, **11**, 122-136.

[15] Stewart, I.D. (2019) Why Should Urban Heat Island Researchers Study History? *Urban Climate*, **30**, Article 100484. https://doi.org/10.1016/j.uclim.2019.100484

[16] He, B., Zhu, J., Zhao, D., Gou, Z., Qi, J. and Wang, J. (2019) Co-Benefits Approach: Opportunities for Implementing Sponge City and Urban Heat Island Mitigation. *Land Use Policy*, **86**, 147-157. https://doi.org/10.1016/j.landusepol.2019.05.003

[17] Getis, A. and Ord, J.K. (1992) The Analysis of Spatial Association by Use of Distance Statistics. *Geographical Analysis*, **24**, 189-206. https://doi.org/10.1111/j.1538-4632.1992.tb00261.x

[18] Ord, J.K. and Getis, A. (1995) Local Spatial Autocorrelation Statistics: Distributional Issues and an Application. *Geographical Analysis*, **27**, 286-306. https://doi.org/10.1111/j.1538-4632.1995.tb00912.x

[19] Mitchell, A. (2005) The ESRI Guide to GIS Analysis, Volume 2: Spatial Measurements and Statistics. ESRI Press.

[20] Chen, G., Iwasaki, T., Qin, H. and Sha, W. (2014) Evaluation of the Warm-Season Diurnal Variability over East Asia in Recent Reanalyses JRA-55, Era-Interim, NCEP CFSR, and NASA Merra. *Journal of Climate*, **27**, 5517-5537. https://doi.org/10.1175/jcli-d-14-00005.1

[21] Ampofo, S., Zakaria, H. and Ahmed, A. (2018) Land Use/Land Cover Change and Urban Heat Island Intensity in the Accra Metropolitan Area, Ghana. *Ethiopian Journal of Environmental Studies and Management*, **11**, 525-539.

[22] Awuh, M.E., Japhets, P.O., Officha, M.C., Okolie, A.O. and Enete, I.C. (2019) A Correlation Analysis of the Relationship between Land Use and Land Cover/Land Surface Temperature in Abuja Municipal, FCT, Nigeria. *Journal of Geographic Information System*, **11**, 44-55. https://doi.org/10.4236/jgis.2019.111004

[23] Feyisa, G.L., Dons, K. and Meilby, H. (2014) Efficiency of Parks in Mitigating Urban Heat Island Effect: An Example from Addis Ababa. *Landscape and Urban Planning*, **123**, 87-95. https://doi.org/10.1016/j.landurbplan.2013.12.008

[24] Guerri, G., Crisci, A., Messeri, A., Congedo, L., Munafò, M. and Morabito, M. (2021) Thermal Summer Diurnal Hot-Spot Analysis: The Role of Local Urban Features Layers. *Remote Sensing*, **13**, Article 538. https://doi.org/10.3390/rs13030538

[25] Ghanghermeh, A., Roshan, G., Asadi, K. and Attia, S. (2024) Spatiotemporal Analysis of Urban Heat Islands and Vegetation Cover Using Emerging Hotspot Analysis in a Humid Subtropical Climate. *Atmosphere*, **15**, Article 161. https://doi.org/10.3390/atmos15020161

[26] Degefu, M.A., Argaw, M., Feyisa, G.L. and Degefa, S. (2021) Effects of Urbanization on the Relationship between Greenspace Patterns and Evolution of Regional Heat Island in Cities of Ethiopia. *Chinese Journal of Population, Resources and Environment*, **19**, 330-343. https://doi.org/10.1016/j.cjpre.2022.01.006

[27] Diffenbaugh, N.S. and Giorgi, F. (2012) Climate Change Hotspots in the CMIP5 Global Climate Model Ensemble. *Climatic Change*, **114**, 813-822. https://doi.org/10.1007/s10584-012-0570-x

[28] Zhibin, R., Haifeng, Z., Xingyuan, H., Dan, Z. and Xingyang, Y. (2014) Estimation of the Relationship between Urban Vegetation Configuration and Land Surface Temperature with Remote Sensing. *Journal of the Indian Society of Remote Sensing*, **43**, 89-100. https://doi.org/10.1007/s12524-014-0373-9

[29] Mohamed, A., Lorestani, N. and Shabani, F. (2025) Impact of Urbanization on Land Surface Temperature: A Global Perspective. *Current Research in Environmental Sustainability*, **10**, Article 100315. https://doi.org/10.1016/j.crsust.2025.100315

[30] Zhou, D., Xiao, J., Bonafoni, S., Berger, C., Deilami, K., Zhou, Y., *et al.* (2019) Satellite Remote Sensing of Surface Urban Heat Islands: Progress, Challenges, and Perspec-

tives. *Remote Sensing*, **11**, Article 48. https://doi.org/10.3390/rs11010048

[31] Adeyemi, A., Botai, J., Ramoelo, A., Van der Merwe, F. and Tsela, P. (2015) Effect of Impervious Surface Area and Vegetation Changes on Mean Surface Temperature over Tshwane Metropolis, Gauteng Province, South Africa. *South African Journal of Geomatics*, **4**, 351-368. https://doi.org/10.4314/sajg.v4i4.1

[32] Worku, G., Teferi, E. and Bantider, A. (2021) Assessing the Effects of Vegetation Change on Urban Land Surface Temperature Using Remote Sensing Data: The Case of Addis Ababa City, Ethiopia. *Remote Sensing Applications: Society and Environment*, **22**, Article 100520. https://doi.org/10.1016/j.rsase.2021.100520

[33] Liu, S., Li, X., Shi, Z., Geng, M., Yu, G. and Hu, T. (2025) Urbanization Is Projected to Increase Local Surface Temperature by 2100. *Communications Earth & Environment*, **6**, Article No. 988. https://doi.org/10.1038/s43247-025-02947-1

[34] Enete, I.C., Awuh, M.E. and Amawa, S. (2014) Assessment of Health Related Impacts of Urban Heat Island (UHI) in Douala Metropolis, Cameroon. *International Journal of Environmental Protection and Policy*, **2**, 35-40. https://doi.org/10.11648/j.ijepp.20140201.15

[35] Oliveira, S., Andrade, H. and Vaz, T. (2011) The Cooling Effect of Green Spaces as a Contribution to the Mitigation of Urban Heat: A Case Study in Lisbon. *Building and Environment*, **46**, 2186-2194. https://doi.org/10.1016/j.buildenv.2011.04.034

[36] Weng, Q., Lu, D. and Schubring, J. (2004) Estimation of Land Surface Temperature–vegetation Abundance Relationship for Urban Heat Island Studies. *Remote Sensing of Environment*, **89**, 467-483. https://doi.org/10.1016/j.rse.2003.11.005

[37] Eshetie, S.M. (2024) Exploring Urban Land Surface Temperature Using Spatial Modelling Techniques: A Case Study of Addis Ababa City, Ethiopia. *Scientific Reports*, **14**, Article No. 6323. https://doi.org/10.1038/s41598-024-55121-6

[38] Ali, A.A.B., Mitra, C. and Rahaman, S.K.N. (2025) Mapping the Heat with Spatial Trends and Emerging Temperature Hotspots in the Contiguous U.S. (CONUS) Counties from 2000 to 2022. *Spatial Information Research*, **33**, Article No. 35. https://doi.org/10.1007/s41324-025-00634-z

[39] Varela, R., de Castro, M., Dias, J.M. and Gómez-Gesteira, M. (2023) Coastal Warming under Climate Change: Global, Faster and Heterogeneous. *Science of the Total Environment*, **886**, Article 164029. https://doi.org/10.1016/j.scitotenv.2023.164029

[40] Buyantuyev, A. and Wu, J. (2010) Urban Heat Islands and Landscape Heterogeneity: Linking Spatiotemporal Variations in Surface Temperatures to Land-Cover and Socioeconomic Patterns. *Landscape Ecology*, **25**, 17-33. https://doi.org/10.1007/s10980-009-9402-4

[41] WHO (2015) Heatwaves and Health: Guidance on Warning-System Development? World Meteorology Organization.

[42] Mora, C., Counsell, C.W.W., Bielecki, C.R. and Louis, L.V. (2017) Twenty-Seven Ways a Heat Wave Can Kill You: *Circulation: Cardiovascular Quality and Outcomes*, **10**, 1-3. https://doi.org/10.1161/circoutcomes.117.004233

[43] Mrema, S., Shamte, A., Selemani, M. and Masanja, H. (2012) The Influence of Weather on Mortality in Rural Tanzania: A Time-Series Analysis 1999-2010. *Global Health Action*, **5**, Article 19068. https://doi.org/10.3402/gha.v5i0.19068

[44] Omonijo, A.G., Adeofun, C.O., Oguntoke, O. and Matzarakis, A. (2012) Relevance of Thermal Environment to Human Health: A Case Study of Ondo State, Nigeria. *Theoretical and Applied Climatology*, **113**, 205-212. https://doi.org/10.1007/s00704-012-0777-9

[45] Njoku, C.A. and Daramola, M.T. (2019) Human Outdoor Thermal Comfort Assessment in a Tropical Region: A Case Study. *Earth Systems and Environment*, **3**, 29-42. https://doi.org/10.1007/s41748-019-00090-4

[46] Ndetto, E.L. and Matzarakis, A. (2017) Assessment of Human Thermal Perception in the Hot-Humid Climate of Dar Es Salaam, Tanzania. *International Journal of Biometeorology*, **61**, 69-85. https://doi.org/10.1007/s00484-016-1192-1